JGR Oceans

RESEARCH ARTICLE
10.1029/2020JC016374

Key Points:
- Long-term freshening of Antarctic Bottom Water was detected off Cape Darnley, East Antarctica, from the 1970s to 2016
- To the west warming was detected near the bottom of the northern basin, while freshening was prominent on the continental slope
- The freshening signal spread along the upper continental slope, which may feed excess freshwater into the abyssal Weddell Gyre

Correspondence to:
S. Aoki,
shigeru@lowtem.hokudai.ac.jp

Citation:
Aoki, S., Katsumata, K., Hamaguchi, M., Noda, A., Kitade, Y., Shimada, K., et al. (2020). Freshening of Antarctic bottom water off Cape Darnley, East Antarctica. *Journal of Geophysical Research: Oceans*, *125*, e2020JC016374. https://doi.org/10.1029/2020JC016374

Received 9 MAY 2020
Accepted 29 JUN 2020
Accepted article online 1 JUL 2020

Freshening of Antarctic Bottom Water Off Cape Darnley, East Antarctica

S. Aoki[1,2], K. Katsumata[3], M. Hamaguchi[2,4], A. Noda[2,5], Y. Kitade[6], K. Shimada[6], D. Hirano[1,2,7], D. Simizu[8], Y. Aoyama[8], K. Doi[8], and Y. Nogi[8]

[1]Institute of Low Temperature Science, Hokkaido University, Sapporo, Japan, [2]Graduate School of Environmental Science, Hokkaido University, Sapporo, Japan, [3]Japan Agency for Marine-Earth Science and Technology, Yokosuka, Japan, [4]Now at C's Lab, Sapporo, Japan, [5]Now at MEXT, Tokyo, Japan, [6]Tokyo University of Marine Science and Technology, Tokyo, Japan, [7]Arctic Research Center, Hokkaido University, Sapporo, Japan, [8]National Institute of Polar Research, Tachikawa, Japan

Abstract Recently, a source of Antarctic Bottom Water (AABW) was identified off Cape Darnley at the eastern end of the Weddell-Enderby Basin. However, the behavior and long-term variability of Cape Darnley Bottom Water (CDBW) are not clearly understood. Hydrographic observations from 1974 to 2016 were compared, and a decade-long bottom temperature record was analyzed to clarify multidecadal changes in the CDBW in this region and its downstream influences. In the Cooperation Sea, CDBW spread northwestward with its deepest part reaching to approximately 4,900 dbar. CDBW freshening of 0.001–0.003 decade^{-1} was revealed. In the Cosmonaut Sea, long-term AABW warming of approximately 0.01–0.03°C decade^{-1} was prominent in the deep basin, while freshening was detected on the upper continental slope. Spatial patterns suggest that an interbasin deep transport of excess freshwater is carried by CDBW and fed into the Weddell Gyre, which might act as an abyssal freshwater buffer.

Plain Language Summary Global oceans' abyss is filled with the cold, dense water fed from the Antarctic coastal margin. The Weddell Sea is the most voluminous supplier of this bottom water. In addition to the well-known source of the bottom water, new source regions are discovered recently: Continental shelf off Cape Darnley, East Antarctica, is one of such regions. Vast parts of the ocean around Antarctica is experiencing freshening for these decades, possibly related to an accelerating ice mass discharge from the Antarctic continent. In contrast, the abyssal Weddell Sea has been known to be warming significantly, acting like a huge heat buffer. Our study shows the newly discovered bottom water off Cape Darnley is carrying an increasing amount of freshwater and feeding the excess freshwater into the abyssal Weddell Sea. This suggests that the Weddell Sea experiences changes that originate from a distant, continental source.

1. Introduction

Under the present climate, cold and dense water on the continental shelf around Antarctica feeds the abyssal waters of the global oceans to produce Antarctic Bottom Water (AABW; Orsi et al., 1999). While the southwestern continental shelf of the Weddell Sea is recognized as the major source region that provides the most voluminous varieties of AABW, the shelf regions of the Ross Sea and Adélie Land coast are also known for substantial bottom water production (Rintoul, 1998). In addition to these major sources, recent direct measurements have revealed the formation of AABW from the continental shelves off Cape Darnley and Vincennes Bay, East Antarctica (Kitade et al., 2014; Ohshima et al., 2013).

The abyss off Cape Darnley in the Cooperation Sea is located at the eastern margin of the Weddell-Enderby Basin (WEB), acting as a junction between AABWs from different sources (Figure 1 inset). While the major source of Cape Darnley Bottom Water (CDBW) has been attributed to the outflow of dense shelf water from the Cape Darnley Polynya (CDP; Ohshima et al., 2013; Hirano et al., 2015; Figure 1 inset, red arrow), outflow from the Amery Basin also contributes (Williams et al., 2016). Westward flowing AABW from the Australian-Antarctic Basin (AAB) through the Princess Elizabeth Trough (PET; Figure 1 inset, blue arrow) supplies water at an AABW density class which acts as a precursor and provides ambient bottom water for CDBW (Heywood et al., 1999; Orsi et al., 1999). The CDBW generally advects westward (Jacobs & Georgi, 1977; Meijers et al., 2010) and feeds abyssal water in the Cosmonaut Sea at the density class of

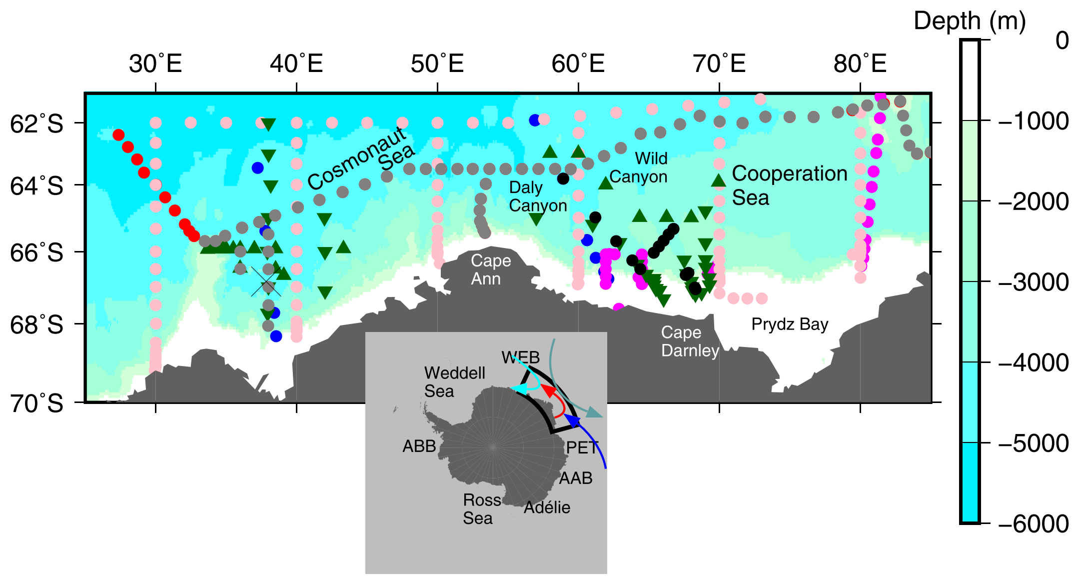

Figure 1. The study area and station locations in the Indian Ocean sector. The inset shows the location of the study area with black square. Symbols denote hydrographic stations in 1974 (blue circle; Conrad), 1996 (red circle, NBP9603), 2008 (green inverted triangle; UM0708), 2009 (green triangle/cyan; UM0809), 2013 (gray; MR12–05), and 2016 (black; KH-16). The white cross at about 38°E, 67°S denotes the location of the bottom temperature mooring. In the inset, WEB is Weddell-Enderby Basin, PET is Princess Elizabeth Trough, AAB is Australia-Antarctic Basin, and ABB is Amundsen-Bellingshausen Basin. Cape Darnley Bottom Water originates from the Cape Darnley Polynya (red arrow), mixed with the westward flowing Antarctic Bottom Water from the AAB through the Princess Elizabeth trough (PET; blue arrow). Weddell Sea deep water recirculates at the eastern margin of the Weddell Gyre (cyan arrow). To the north, the Antarctic circumpolar current carries AABW eastward from the WEB to AAB (green arrow).

Weddell Sea Deep Water (WSDW; Meredith et al., 2000). The Cosmonaut Sea is considered to be the eastern margin of the Weddell Gyre; hence, recirculating WSDW (Figure 1 inset, cyan arrow) mixes with the incoming CDBW here (Schröder & Fahrbach, 1999). To the north of the Weddell Gyre, the Antarctic Circumpolar Current (ACC) carries AABW eastward from the WEB to AAB (Figure 1 inset, green arrow) (Gordon, 1975; Orsi et al., 1999).

Prominent and long-term changes in the properties of AABW have been found in the Southern Ocean (e.g., Aoki et al., 2013, 2005; Azaneu et al., 2013; Fahrbach et al., 2011; Jacobs & Giulivi, 2010; Johnson et al., 2008; Meredith et al., 2008; Purkey & Johnson, 2010, 2013; Rintoul, 2007), and some of these changes have been shown to be accelerating (e.g., Menezes et al., 2017; van Wijk & Rintoul, 2014). While overall warming- and freshening-driven density decreases and layer thinning have been observed for AABW, there are significant regional characteristics among the different basins which are likely to reflect different but interrelated mechanisms. The AABW of the Weddell Sea origin shows significant warming (~0.025°C decade^{-1}) in many regions in the Atlantic Ocean (e.g., Jullion et al., 2010; Meredith et al., 2011; and references therein). In the AAB, van Wijk and Rintoul (2014) described strong freshening diminishing downstream along the pathway of the AABW of the Ross Sea origin; from 0.010 decade^{-1} at 140/150°E to 0.003 decade^{-1} at 80°E and 0.002 decade^{-1} on the southern flank of mid-ocean ridge over the bottom 300 m between the 1970s and 2012. In contrast, warming signal gets stronger; from 0.02°C decade^{-1} at 140/150°E to 0.04°C decade^{-1} at 80°E and southern flank of the ridge. When converted to a change in steric height, Atlantic sector shows a stronger warming contribution compared to the other sectors, while freshening is stronger in the AAB and Amundsen–Bellingshausen Basin as compared to the WEB (Purkey & Johnson, 2013).

On the upper continental slope of the eastern Weddell Gyre, Couldrey et al. (2013) found significant warming of ~0.1°C and a density decrease of 0.02–0.03 kg m^{-3} during 1993–2008 for the AABW variety entering from the east. They attributed this to changes in the properties of CDBW caused by increased entrainment of Circumpolar Deep Water (CDW). However, the discussion of multidecadal changes of CDBW was limited and their subsequent downstream influence was not investigated.

Table 1
List of CTD Observation Used in This Study

Cruise designator	Period	Platform	Publication, if available
Conrad	Jan–Mar 1974	R/V *Conrad*	Jacobs & Georgi (1977)
NBP9603	May–July 1996	R/V *Nathaniel B. Palmer*	
KAOS	Jan–Feb 2003	RSV *Aurora Australis*	
BROKE-West	Jan–Mar 2006	RSV *Aurora Australis*	Meijers et al. (2010)
UM0708	Jan 2008	R/TV *Umitaka maru*	
UM0809	Jan 2009	R/TV *Umitaka maru*	
MR12–05	Jan–Feb 2013	R/V *Mirai*	Uchida et al. (2015)
KH-16	Feb 2016	R/V *Hakuho maru*	
WHP I6			
35MFCIVA_1	Feb 1993	R/V *Marion Dufresne*	Archambeau et al. (1998)
35MF103_1	Mar 1996	R/V *Marion Dufresne*	
33RR20080204	Feb–Mar 2008	R/V *Roger Revelle*	

Based on high-quality top-to-bottom hydrographic observations from 1974–2016, this study focuses on the spatial distribution and long-term changes of CDBW. Together with a bottom temperature record during 2005–2016, the influence of changes in CDBW to the abyssal Weddell Gyre is also investigated.

2. Study Area and Data Sources

We focused on the pathway and long-term changes in CDBW in the Cooperation and Cosmonaut Seas (Figure 1). High-quality top-to-bottom conductivity-temperature-depth (CTD) observations between 30°E and 80°E were used for the post World Ocean Circulation Experiment (WOCE) era (Table 1). In these data, WHP I6 data along 30°E were examined for the upper continental slope. WHP I6 data were low-pass filtered by a 30-dbar median filter. For St.17 of KH-16 in Wild Canyon where a transient signal was found, 5-dbar box-car filter was applied for temperature and salinity profiles. Potential temperature (Bryden, 1973; Fofonoff & Millard, 1983) and the PSS-78 salinity scale were used. Temperature, salinity, and pressure were observed using Seabird Scientific CTDs after 2003. The accuracy of these measurements meets the WOCE standards of 0.002, 0.002°C, and 3 dbar for salinity, temperature, and pressure, respectively. Velocity profiles were measured using a lowered-acoustic Doppler current profiler (L-ADCP) and processed according to Thurnherr et al. (2010) for the MR12–05 and KH-16 cruises. L-ADCP data of BROKE-West cruise (Meijers et al., 2010) were also used. Density values were expressed as neutral density, γ^n.

High-quality historical observations from January (offshore of Cape Darnley) to March (along ~38°E) in 1974 by R/V *Conrad* (Jacobs & Georgi, 1977) were also used. Salinity-temperature-depth sensors of Plessey 9,006 and 9,040 were used. Measurement accuracy was reported as 0.005, 0.01°C, and 10 m for salinity, temperature, and depth, respectively. Every cast was towed within 20 m from the bottom with an average height of 7.4 m off the bottom for the cruise. There are some salinity spikes in the original data. Below the salinity maximum layer where we are interested in, salinity outliers whose difference between the neighboring bottles for the same cast exceeding more than 0.005 were excluded. Only less than 5% of the entire *Conrad* data were removed by this procedure.

In the Cosmonaut Sea at 37°50′E, 66°51′S at an approximate depth of 4,600 dbar, moored temperature observations were conducted by a thermometer attached to the frame of the bottom pressure gauge (Hayakawa et al., 2012). Sea-Bird Scientific MicroCATs were used almost continuously from 16 December 2004 to 14 February 2016. Continuous records were retrieved with exceptions of two gaps of ~10 months (February–December 2006) and 7 days (February 2013). These data gaps were substituted with the less accurate data from the thermistor attached to the bottom pressure gauge. The temperature scale was given in ITS-90.

3. Results

3.1. CDBW Pathway and Mixing Among AABWs

Spatial structure of AABW property in the Cooperation and Cosmonaut Seas is complex, reflecting the different origins and mixing processes of bottom waters in this region. CDBW flows onto the AABW variety coming from the east, mixes with the AABW variety coming from the west (WSDW), and modifies its properties.

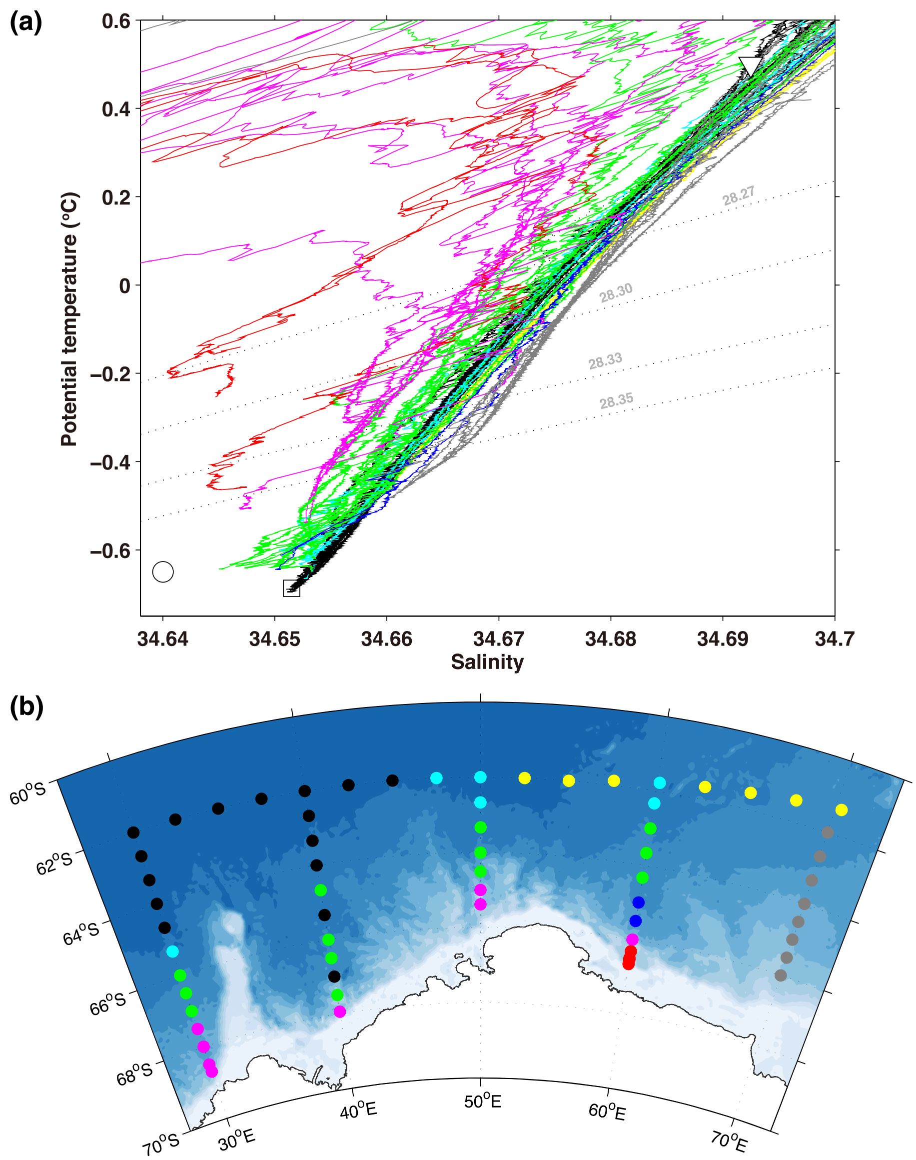

Figure 2. (a) Potential temperature-salinity diagram for BROKE-West section between 30°E and 70°E and (b) distribution of data points with information of varieties of the AABW. Dashed black lines in (a) denote neutral density contours with values shown in gray numerals. Colors denote different fraction of CDBW for bottom 300 dbar average property, calculated based on the three endmembers of CDBW (○), WSDW (□), and LCDW (▽). Cyan indicates the point where CDBW fraction is more than 1% but less than 10%, green above 10%, and magenta the largest fraction among the three endmembers. Red is a transient region where the signal does not fall within the three-endmember triangle. Blue points indicate the point where the fresh signal is seen near the bottom, but vertical average does not show significant CDBW fraction. Gray indicates saltier AABW through the PET. Black denotes that the WSDW fraction is more than 90% and CDBW fraction is less than 1%. Yellow denotes AABW carried by the ACC that do not fall into other categories. See text in details.

To estimate the evolution and mixing processes quantitatively, the contribution of the AABWs are calculated as the mixture among CDBW, WSDW, and Lower-Circumpolar Deep Water (LCDW) using temperature and salinity, based on the BROKE-West CTD data (Figure 2). Fractions of each AABW are calculated for the temperature and salinity averaged over a 300-dbar layer from the bottom. We use the potential temperature and salinity of each endmember as −0.65°C, 34.64 for CDBW, −0.69°C, 34.652 for WSDW, and 0.50°C, 34.693 for LCDW, respectively (CDBW endmember is determined based on Ohshima et al., 2013, and WSDW and LCDW end members are based on the potential temperature-salinity diagram Figure 2 of this study).

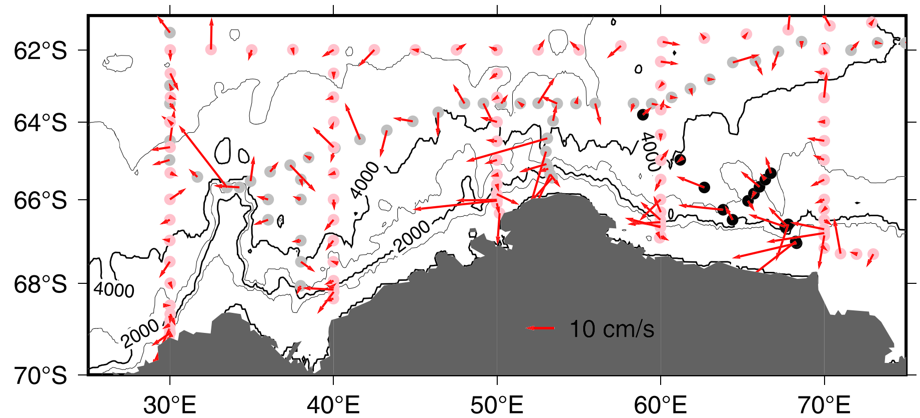

Figure 3. Spatial distribution of bottom velocity vectors. Velocity vectors are averaged for the 50-m-thick layer above the bottom, derived for the BROKE-West (pink dots), MR12-05 (gray dots), and KH16-1 (black dots) cruises.

Colors in Figure 2 indicate the different fraction of CDBW. Cyan indicates the point where CDBW fraction is more than 1% but less than 10%, green indicates the point where CDBW fraction is above 10%, and magenta indicates the point where CDBW is greater than 10% and most dominant. Red falls out of the endmember triangle, presumably due to transient mixing onto the intermediate depths. Blue indicates the point where the fresher CDBW signal is seen near the bottom but vertical average does not show significant CDBW fraction due to the presence of overlying saltier AABW. Gray indicates the AABW through the PET with a saltier signature, providing older source water for CDBW.

The derived fraction demonstrates the northwestward spread of CDBW and further penetration into the southern part of the Cosmonaut Sea (Figure 2b). On the other hand, the northern limb of the Weddell Gyre carries the vertically more homogeneous WSDW (black; WSDW fraction is more than 90% and CDBW fraction is less than 1%) to the region off Cape Ann from the western and northern corner of the analysis domain (Meijers et al., 2010). This southeastward flowing WSDW mixes with the westward flowing CDBW to produce the AABWs whose properties are intermediate between the two AABW varieties.

The detailed vertical structure of the AABW is reflecting complex mixing among different origins of AABWs. For example, two stations at 60°E, 65°S reveal a strong fresh signal near the bottom and slightly saline signature above likely advected from further east (blue lines in Figure 2a). Nevertheless, overall contrast of the vertical averages between west/lower-slope and east/upper-slope regions is robust (Figure 2b); on the upper-slope region, CDBW reveals the highest fraction of 45–70%. The deeper basin is occupied by more than 90% of WSDW in the Cosmonaut Sea.

The westward spread of CDBW and subsequent mixing is indicated by the distribution of the bottom velocity field as well. The spatial distribution of the bottom velocity, averaged over the 50 m layer above the bottom, obtained during 2006 and 2016 generally supports the pathway derived from the CDBW temperature and salinity signature (Figure 3). The westward flow is generally stronger on the upper slope. Stations that are shallower than ~4,000 dbar generally show a westward velocity along isobaths. We note here that tides are weak in this region (e.g., Padman et al., 2018). Detailed flow structure of KH-16 indicate that the dense water descended the Wild Canyon, circulated westward along the spur, and then spread equatorward and westward in the Daly Canyon. Given a typical speed of 0.1 m s^{-1}, derived by the L-ADCP and previous mooring record (Ohshima et al., 2013), newly-ventilated CDBW takes several months to traverse the Wild/Daly Canyons.

3.2. Long-Term Variability of CDBW and AABW Varieties in the Cooperation Sea

As above, different AABW varieties of different origins exist in this ocean sector. To examine long-term changes in the properties of the CDBW, we examine the differences between observations from 1996 (NBP9603) and 2013 (MR12–05) along WHP S4I (Figure 4). Between 50°E and 62°E (~4,300–4,900 dbar) where the CDBW signature is clear, freshening is significant in waters denser than 28.33 kg m^{-3} (Figures 4b and 4c). The densest water in the 300-dbar-thick layer from the sea bed freshened by 0.002–

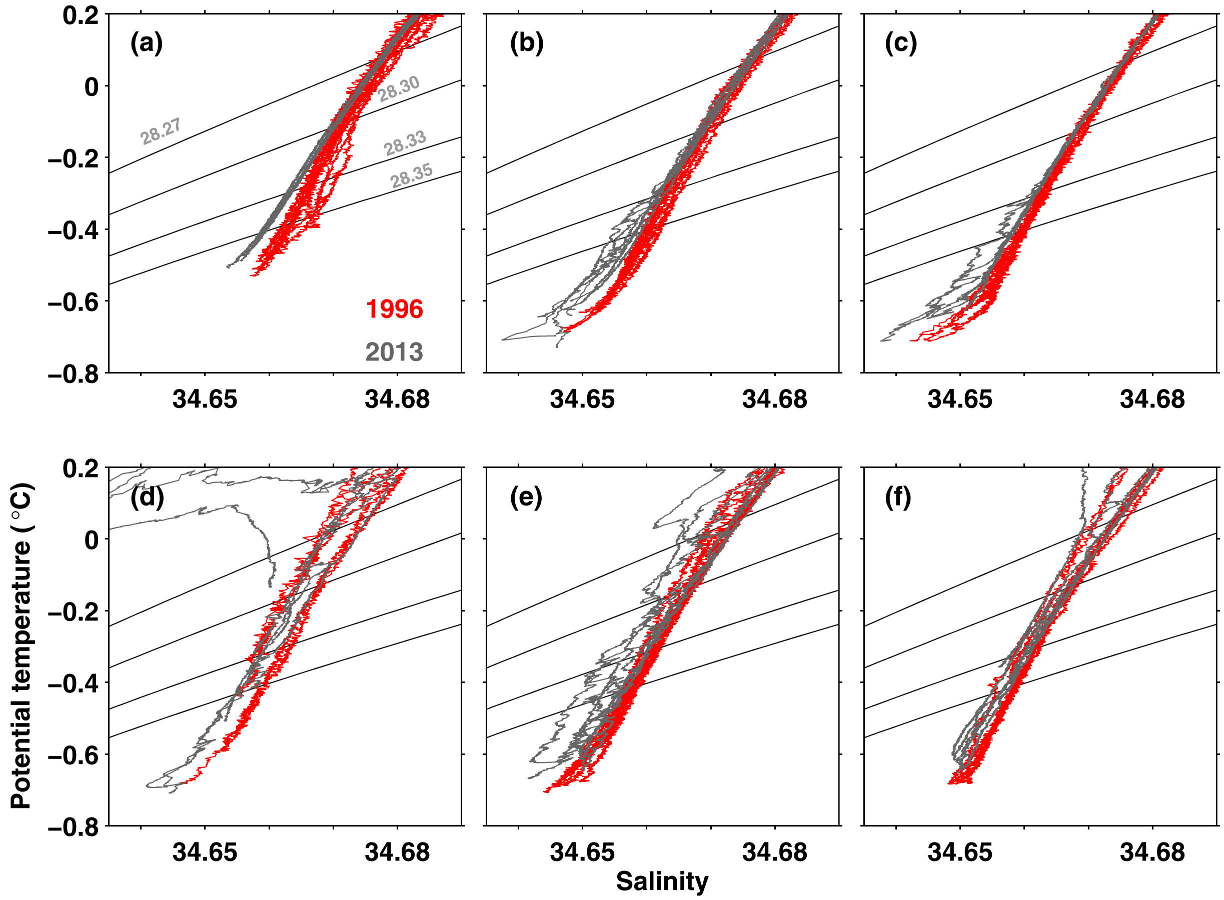

Figure 4. Potential temperature-salinity diagrams in the Cooperation and Cosmonaut Seas along the WHP S4I section for 1996 and 2013 cruises. (a) 62–80°E, (b) 55–62°E, (c) 50–55°E, (d) cross-slope section along 53°E, (e) 40–50°E, (f) 34–40°E. Red lines denote observations in 1996 and gray lines in 2013.

0.003 (0.001–0.002 decade^{-1}; salinity and temperature changes near the bottom are calculated for this layer and averaged among the available stations throughout unless otherwise specified). Temperature changes are not coherent nor significant. The thickness of the layer denser than 28.30 kg m^{-3} (densest layer thickness, hereafter) decreased at 87 ± 57 dbar decade^{-1} west of Cape Darnley between 55°E and 62°E. North of Cape Ann between 50°E and 55°E, density decreases by ~0.01 kg m^{-3} (0.006 kg m^{-3} decade^{-1}) at the bottom, accompanied by freshening (Figure 4c). Along the 53°E section between 66°S and 63.75°S off Cape Ann, freshening of ~0.003 (0.002 decade^{-1}) was detected near the bottom (Figure 4d). Note that seasonal differences in the observation periods between the two WHP S4I occupations may have influenced these differences, especially immediate downstream of Cape Darnley.

To the east of the CDBW pathway north of Cape Darnley and near the PET, freshening of ~0.0018–0.0034 (0.001–0.002 decade^{-1}) and warming of 0.025–0.041°C (~0.02°C decade^{-1}) are observed, with a density decrease of 0.007–0.01 kg m^{-3} (~0.005 kg m^{-3} decade^{-1}; Figure 4a). The densest layer thickness decreases at ~40 dbar decade^{-1}.

Although the positions do not exactly coincide with other stations (except the two revisited stations at 59°E, 64°S and at 53°E, 58°S in 1974 and 2016), some reasonably close stations can be compared over the longer period of 1974–2009/2013/2016 (Figure 5). The property changes are calculated as the difference between the oldest and latest observations unless otherwise specified. The observed changes are roughly consistent with those derived from the WHP S4I observation for the period 1996–2013 shown in Figure 4.

In the Cooperation Sea at 3,800–4,100 dbar in the Daly Canyon (61°E, 65°S), the densest water freshened by 0.015 from 1974 to 2016 (0.0035 decade^{-1}; Figure 5a). Warming of 0.02°C (0.0047°C decade^{-1}) is associated

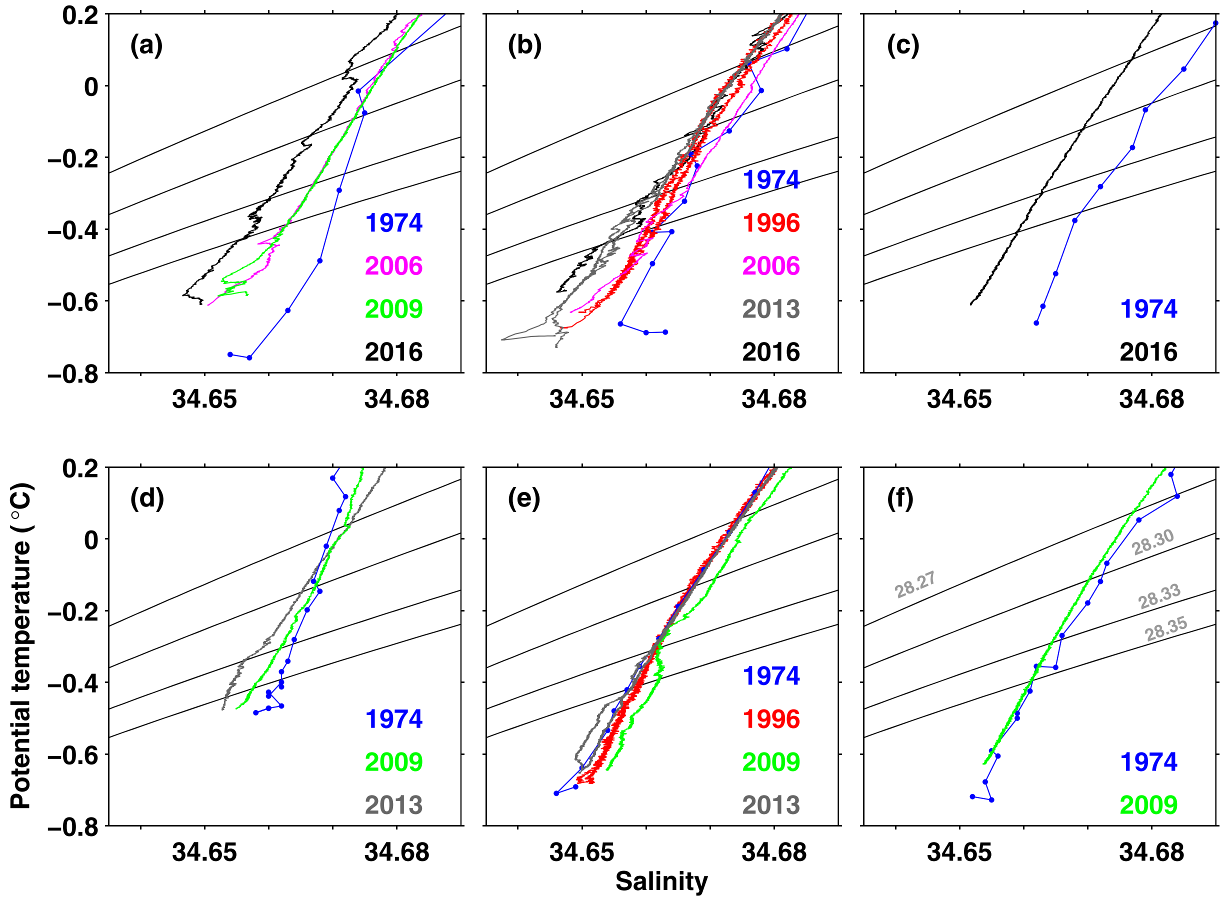

Figure 5. Potential temperature-salinity diagrams in the Cooperation Sea (a–c) and Cosmonaut Sea (d–e) for observations during 1974–2016. (a) 61°E, 65°S, (b) 59°E, 64°S, (c) 53°E, 58°S, (d) 38°E, 68°S, (e) 38°E, 65°S, and (f) 38°E, 60°S. Lines are colored with respect to years.

with a lightening of density by 0.037 kg m^{-3} (0.009 kg m^{-3} decade^{-1}). The densest layer thickness decreased at 50 dbar decade^{-1}. Slightly offshore at 59°E, 64°S and ~4,300–4,600 dbar, a bottom freshening of 0.011 (0.0026 decade^{-1}) is apparent between 1974 and 2016 (Figure 5b). Warming of 0.047°C (0.011°C decade^{-1}) lowered density by 0.04 kg m^{-3} (0.01 kg m^{-3} decade^{-1}); however, a significantly cooler anomaly around −0.7°C is apparent in 2013 which is comparable to 1974 temperatures and suggests a presence of large interannual variability.

On the upper slope at 66.5°S and ~2,700 dbar, the densest water freshened by ~0.006 from 2003 to 2016 (0.0046 decade^{-1}; Figure 6a). No high-quality historical observations are available in the Wild Canyon; however, 7-year differences between 2009 and 2016 show fresher anomalies of ~0.02 near the bottom (Figure 6b). Comparisons between stations further up on the slope (at 9 km horizontal distance and 500-dbar difference; 900 and 1,400 dbar, respectively) reveals a freshening of 0.014 (Figure 6c). The freshening signal can be traced upward to the salinity maximum (core of LCDW; not shown). Although the uncertainty from interannual variability and spatial sampling difference is large, these comparisons do not contradict with the long-term freshening signal near the bottom off Cape Darnley. The general freshening signal is hence consistent with the WHP S4I observations.

3.3. Long-Term Variability of AABW Varieties in the Cosmonaut Sea

In the Cosmonaut Sea at a depth of 4,500–4,900 dbar along WHP S4I (about 65°S), changes in AABW between observations from 1996 to 2013 differ as compared to the changes in the Cooperation Sea. Warming is distinct while no obvious salinity change is seen (Figure 4f). The densest water warms at ~0.04–0.06°C (~0.03°C decade^{-1}), associated with a density decrease of 0.01–0.012 kg m^{-3} (0.006–

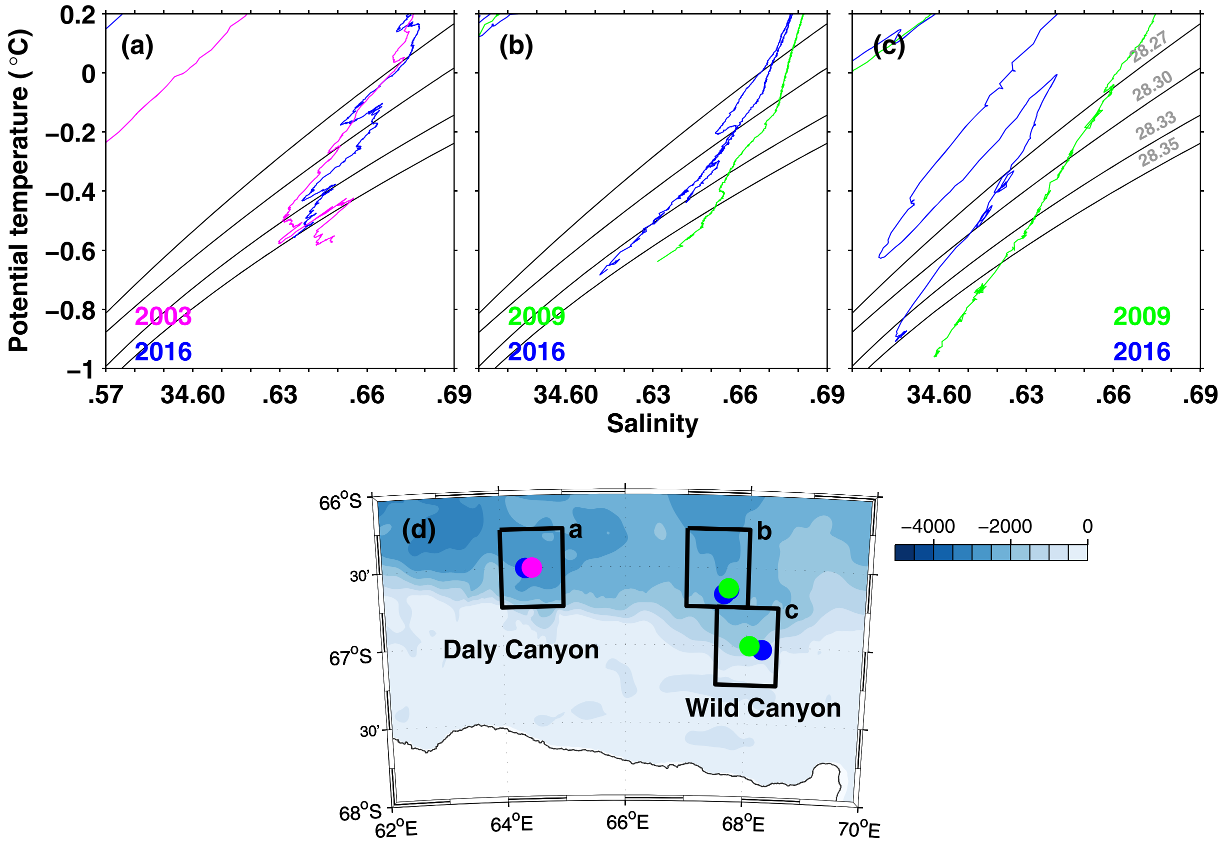

Figure 6. Potential temperature-salinity diagrams in the Cooperation Sea during 2003–2016. Data at the (a) upper continental slope in Daly Canyon, (b) upper continental slope in Wild Canyon, and (c) uppermost slope in the canyon. (d) Spatial distribution of the data (circle). Lines and circles are colored with respect to years.

0.007 kg m^{-3} decade^{-1}). The densest layer thickness decreases at ~74–135 dbar decade^{-1} resulting in a deepening of dense isopycnals, which are generally larger than the layer thickness change observed in the Cooperation Sea.

Along about 38°E, long-term properties over the longer period of 1974–2016 differ from those of the Cooperation Sea as well. On the upper slope at approximately 68°S and 3,800–4,200 dbar, freshening of ~0.007 (0.002 decade^{-1}) is apparent between 1974 and 2013; however, only a small temperature change is observed (Figure 5d). In a deeper region at approximately 65°S and 4,900 dbar, warming of ~0.056°C (0.014°C decade^{-1}) occurred between 1974 and 2013, while no significant salinity tendency is apparent (Figure 5e). At the deepest point (60°S and 5,100–5,400 dbar), a more distinct warming of ~0.099°C (0.028°C decade^{-1}) was observed between 1974 and 2009 (Figure 5f). A decrease in bottom density is also apparent (0.020 kg m^{-3} or 0.0056 kg m^{-3} decade^{-1}), with the 28.30 kg m^{-3} isopycnal surface lowering by 136 dbar decade^{-1}. Hence, the warming signal increases toward north, while freshening signal is present on the continental slope region.

Further west along the southern end of the 30°E line, a change in salinity is also detected (Figure 7). At a few stations on the upper continental slope of 3,100–3,500 dbar where CFC maximum is located (Archambeau et al., 1998), a freshening of 0.003 is observed from 1993 to 2006 for AABW around a density of 28.34 kg m^{-3} (Figure 7a). The freshening signal is less prominent on the slightly deeper continental slope (Figure 7b) and not detected at depths exceeding 5,000 dbar (Figure 7c), while warming signal is prominent (Couldrey et al., 2013). Hence, the freshening signal is detected on the upper continental slope, in a somewhat confined area.

Multidecadal comparisons show generally consistent variations of warming along WHP S4I section at ~65°S. Hence, in the Cosmonaut Sea, the warming signature intensifies from the upper slope (68°S ~4,000 dbar) to

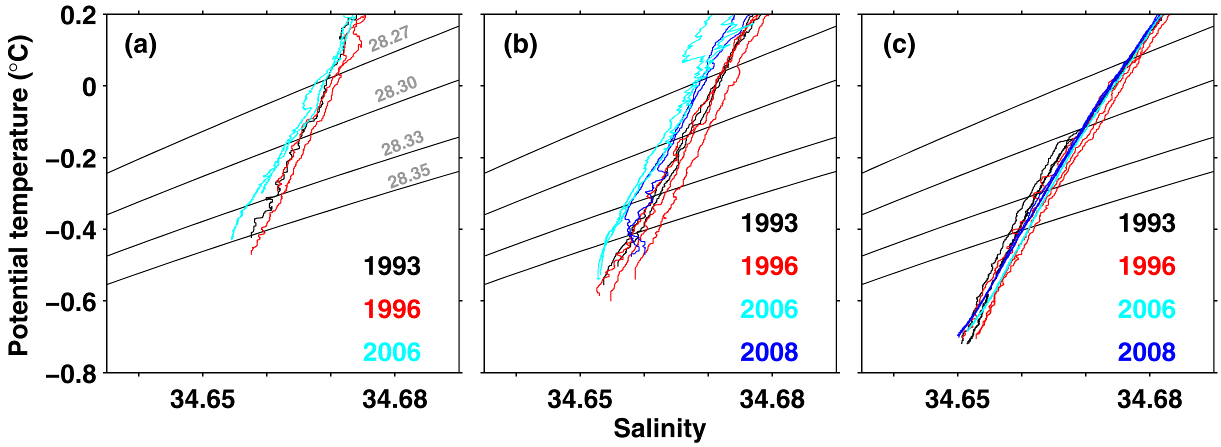

Figure 7. Potential temperature-salinity diagrams along the WHP I6 line (30°E) during 1993–2008. Data at the (a) uppermost continental slope at ~68.5°S, (b) upper slope between 67–68°S, and (c) deep basin between 61.5°S and 63°S.

the deeper basin (60°S ~5,000 dbar), while the freshening signal is found but confined on the upper continental slope. The meridional structure is consistent with that found further west along 30°E.

3.4. Bottom Temperature Time Series in the Cosmonaut Sea

A time series of bottom temperatures at 38°E, 67°S and ~4,600 dbar shows a gradual warming, with a linear trend of 0.0071 ± 0.0011°C decade^{-1} (two-tailed 95% interval; Figure 8). The warming rate is consistent with those found to the north and south; smaller than the 0.01–0.03°C decade^{-1} warming for the 60–65°S region during 1974–2013 (Figures 4f and 5e) and larger than the negligible temperature change at ~68°S (Figure 5d). The north-south contrast likely reflects the spatial structure of a stronger warming toward the gyre interior as mentioned in section 3.3. The warming rate is close to the value detected in the interior of the Weddell Gyre along the Prime Meridian [Fahrbach et al., 2011; their Figure 5d], although there is significant decadal variability in the Weddell Gyre.

Although the warming trend is statistically significant, the time series also exhibits a significant interannual (~6–8 years scale) variability, with highs during 2007–2011 and 2015–2016 and lows during 2006 and 2012–2013. This fact suggests a complex nature of the water properties and limitation of observations over only several years in interpreting the long-term trend. For example, two samplings of 6 or 7 years apart from 2006 summer yield warmer change while that from 2008 summer yield cooler change. Hence, it highlights

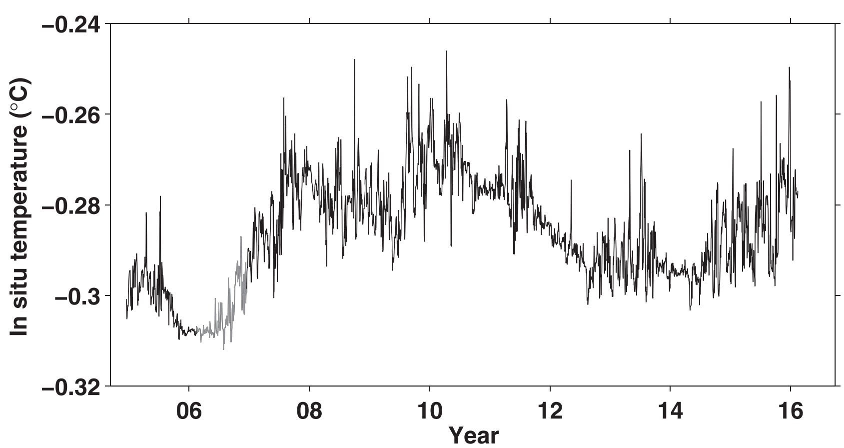

Figure 8. Time series of in situ temperatures (°C) of bottom pressure gauges during 2005–2016 at 37°50′E, 66°51′S in the Cosmonaut Sea. The gray line indicates gap periods where data were substituted with temperatures derived from the sensor attached to the pressure gauge.

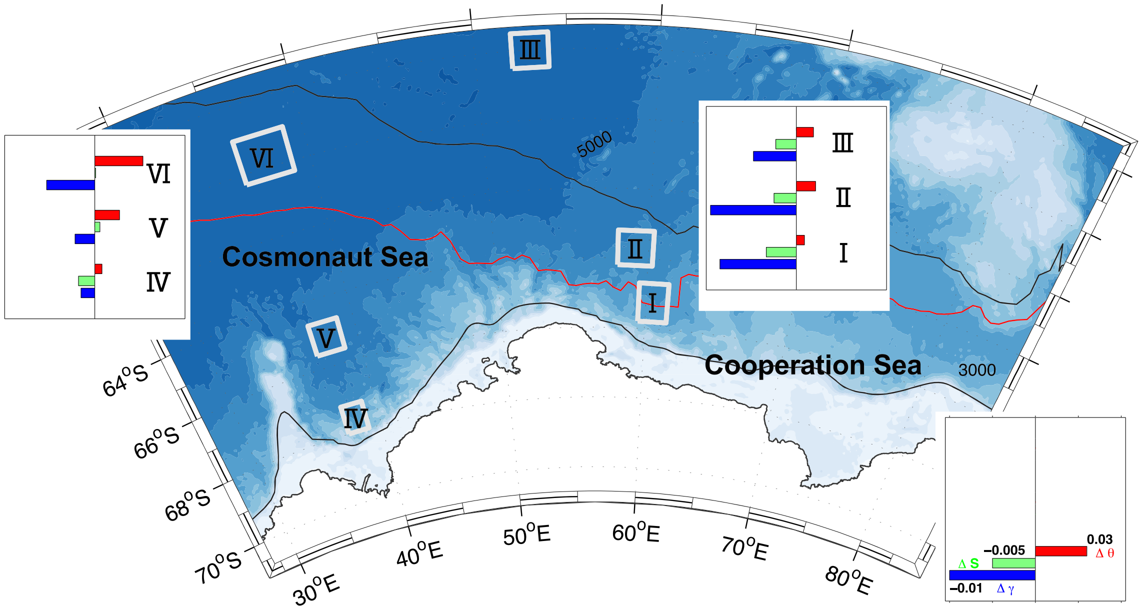

Figure 9. Summary of salinity and temperature trends in the Cooperation and Cosmonaut Seas. Bar charts show the difference between 1974 and 2016 of potential temperature (red) and salinity (green) for the densest water (averaged at 300 dbar above the bottom) and of bottom neutral density (blue) for the Cosmonaut Sea (left) and Cooperation Sea (right) at the location indicated by Roman numeral. The bar chart on the lower-right corner indicates an arbitrary change for each variable as a reference scale.

the need of a long-term difference at least more than 10 years, although the rate may still depend on the chosen period. Thus, the warming signal obtained from our 11-year record lends support for the basin-scale warming in the Cosmonaut Sea.

4. Discussion

4.1. Source of CDBW Freshening

The meridional pattern of salinity and temperature changes in the Cooperation and Cosmonaut Seas are summarized in Figure 9. CDBW freshening of 0.001–0.003 decade^{-1} was observed in the Cooperation Sea while AABW warming is evident in the Cosmonaut Sea. However, a freshening signal is also evident along the upper slope in the WEB as well. As the Cooperation Sea is the junction between the WEB and AAB, the pattern is consistent with the observed spatial patterns of the warming (strongest in the WEB; Meredith et al., 2008) and freshening (strongest in the AAB and Amundsen–Bellingshausen Basin; Purkey & Johnson, 2010, 2013).

To determine the source of the freshening of CDBW, the bottom water pathway and formation process should be considered. The Dense Shelf Water (DSW) outflow from the CDP and Prydz Bay mixes with the ambient AABWs. Freshening can be hence attributed to changes in ambient AABWs, which come from both the east and northwest, and/or changes in the processes contributing to the CDBW ventilation and mixing on the continental shelf/slope.

Changes of the ambient AABW from the east can be important. In the PET, a freshening of 0.003 decade^{-1}, warming of 0.03°C decade^{-1}, and density reduction of 0.007 kg m^{-3} decade^{-1} were observed during 1972–2007 (van Wijk & Rintoul, 2014), which are comparable to the observed changes in the CDBW in the Cooperation Sea. These conditions are similar to those off the Adélie Land coast in the AAB, where AABW from the Ross Sea is mixed with the outflow from shelf depressions. The freshwater source is attributed to increasing discharge of continental ice from the West Antarctic (Jacobs & Giulivi, 2010; Vaughan et al., 2013), suggesting that the interbasin transport of freshwater from the AAB could contribute significantly to CDBW freshening.

In addition, freshening and warming signals were detected in the northwest ACC region. At 53°E 58°S, at an approximate depth of 5,300 dbar, a freshening of 0.01 (0.0024 decade^{-1}), warming of 0.04°C

(0.01°C decade^{-1}) and density decrease of 0.02 kg m^{-3} (0.005 kg m^{-3} decade^{-1}) were observed from 1974 to 2016 (Figure 5c) throughout the AABW density range. The θ-S curve to the north and east of this region is fresher and warmer; hence, a southward shift of the ACC (Aoki et al., 2003; Gille, 2002, 2008) can partly explain this change if the vertical structure extends throughout the water column. Another potential source of the changing conditions is the freshening of the endmember of the AABW. For example, in the Drake Passage on the opposite side of the Weddell Gyre, decadal freshening of 0.004 decade^{-1} was observed during 1993–2011 at slightly lighter density range of 28.26–28.31 kg m^{-3} (Jullion et al., 2013). Although the cause of the freshening was not documented, continental ice melt from the Larsen Ice Shelf can be a possible contributor.

Direct observations provide limited evidence to identify the changes contributing to the DSW property and ventilation from the CDP. Schmidko et al. (2014) described a freshening of 0.05 $\pm$ 0.03 decade^{-1} from the 1980s to the 2000s on the shelf. Decreasing trends in sea ice production were reported during 1992–2013 for the CDP (Tamura et al., 2016). Advection of the West Antarctic meltwater is another possible freshwater source (Rye et al., 2014). If the freshening signal is accurate, then shelf water freshening can substantially contribute to the freshening of the CDBW given a mixing ratio of 42:58 of DSW to CDW (Ohshima et al., 2013). However, the paucity of winter observation of DSW makes it difficult to identify the freshening of DSW.

To summarize, the freshening of CDBW is primarily attributed to the westward flowing AABW through PET. However, the AABWs from the west and dense shelf water outflow from the CDP might also contribute to the freshening signal, although it is less conclusive.

4.2. Injection of CDBW Freshening Into the Weddell Gyre

While warming is prominent in the abyssal basin of the Cosmonaut Sea, westward advection of CDBW can transport a freshening signal downstream along the southern limb of the Weddell Gyre. At the upper continental slope (a depth of 3,100–3,600 dbar) along 30°E line, freshening is observed during 1993–2006. The signal is located at the southernmost region of the warming signal (Couldrey et al., 2013) and the core region of newly-ventilated bottom water with CFC maximum (Archambeau et al., 1998). Given the paucity of abyssal ventilation sites from Cape Darnley to 30°E, inferred from the absence of coastal polynya (Nihashi & Ohshima, 2015) and fresh bottom salinity distribution (Schmidko et al., 2014), the freshening signal here can be traced back to the Cooperation Sea. Albeit with significant interannual/decadal variability (Fahrbach et al., 2011, 1998), long-term freshening in the Cooperation Sea is very likely affecting the Weddell Gyre downstream.

During 1993–2008 prominent warming with absence of salinity change was reported for AABW at the CFC maximum on the continental slope along 30°E (Couldrey et al., 2013). Couldrey et al. (2013) attributed this to changes in the properties of CDBW, southward shift of ACC resulting in enhanced entrainment of CDW, and freshening of CDBW source waters. The warming signal is consistent with the CDBW change reported in the present study and subsequent mixing with WSDW. While the observed freshening and lightening of CDBW around 65°E can partly explain the property changes observed along 30°E (freshening of CDBW source waters), the observed warming signal of CDBW in the Cooperation Sea is weaker than those in the Cosmonaut Sea along 38°E, that is, eastern limb of the Weddell Gyre. Warming signal is more evident for WSDW of Weddell Gyre origin, and hence mixing between the recirculating WSDW on the northeastern limb and CDBW might explain the significant warming signal on the upper continental slope.

5. Conclusions

Historical and present high-quality observations demonstrate that AABW freshening is prominent in the Cooperation Sea, while AABW warming is evident in the Cosmonaut Sea. The contrast is consistent with that between Indo-Pacific and Atlantic sectors, which suggests that the signals are competing in this section of the Southern Ocean. Multiple sources of excess freshwater from the Antarctic margin appear to meet in the abyss of the Cooperation Sea.

Interannual variability is prominent in the continuous time series of the bottom temperature record in the Cosmonaut Sea, raising a caution on samplings of only several years apart. Hence, sustained and temporary high-resolution observations are necessary in this area to elucidate highly accurate description of ongoing

AABW changes. This information is essential to understand abyssal injections of the interbasin transport of excess freshwater into the Weddell Gyre system, which possibly acts as a huge freshwater buffer.

Data Availability Statements

Hydrographic data from WHP S4I, KAOS, and BROKE-West are available through CCHDO (https://cchdo.ucsd.edu/). Hydrographic data of UM0708/0809 and KH-16, bottom temperature series are available through NIPR ADS database (https://ads.nipr.ac.jp/dataset/A20200619-001; -002; -003; -004). The LADCP data of BROKE-West were kindly provided by Meijers.

Acknowledgments

The authors thank Ikehara, Moteki, Bindoff, and Church for leading the cruises. We are most grateful to the captains, crews, and colleagues on board R/V *Mirai*, *Hakuho maru*, *Umitaka maru*, and *Aurora Australis*. We are greatly indebted to two anonymous reviewers to an earlier version of the manuscript. This work was supported by Grant-in-Aid for Scientific Research (17H01615) of the MEXT of the Japanese Government.

References

Aoki, S., Kitade, Y., Shimada, K., Ohshima, K. I., Tamura, T., Bajish, C. C., et al. (2013). Widespread freshening in the seasonal ice zone near 140°E off the Adelie Land Coast, Antarctica, from 1994 to 2012. *Journal of Geophysical Research: Oceans*, *118*, 6046–6063. https://doi.org/10.1002/2013JC0090009

Aoki, S., Rintoul, S. R., Ushio, S., Watanabe, S., & Bindoff, N. L. (2005). Freshening of the Adélie Land Bottom Water near 140°E. *Geophysical Research Letters*, *32*, L23601. https://doi.org/10.1029/2005GL024246

Aoki, S., Yoritaka, M., & Masuyama, A. (2003). Multi-decadal warming of subsurface temperature in the Indian sector of the Southern Ocean. *Journal of Geophysical Research*, *108*(C4), 8081. https://doi.org/10.1029/2000JC000307

Archambeau, A. S., Pierre, C., Poisson, A., & Schauer, B. (1998). Distributions of oxygen and carbon stable isotopes and CFC-12 in the water masses of the Southern Ocean at 30°E from South Africa to Antarctica: Results of the CIVA1 cruise. *Journal of Marine Systems*, *17*, 25–38.

Azaneu, M., Kerr, R., Mata, M. M., & Garcia, C. A. E. (2013). Trends in the deep Southern Ocean (1958–2010): Implications for Antarctic bottom water properties and volume export. *Journal of Geophysical Research: Oceans*, *118*, 4213–4227. https://doi.org/10.1002/jgrc.20303

Bryden, H. (1973). New polynomials for thermal expansion, adiabatic temperature gradient and potential temperature of sea water. *Deep Sea Research*, *20*, 401–408.

Couldrey, M. P., Jullion, L., Naveira Garabato, A. C., Rye, C., Herraiz-Borreguero, L., Brown, P. J., et al. (2013). Remotely induced warming of Antarctic bottom water in the eastern Weddell gyre. *Geophysical Research Letters*, *40*, 2755–2760. https://doi.org/10.1002/grl.50526

Fahrbach, E., Hoppema, M., Rohardt, G., Boebel, O., Klatt, O., & Wisotzki, A. (2011). Warming of deep and abyssal water masses along the Greenwich meridian on decadal time scales: The Weddell Gyre as a heat buffer. *Deep-Sea Research Part II*, *58*, 2509–2523. https://doi.org/10.1016/j.dsr2.2011.06.007

Fahrbach, E., Meyer, R., Rohardt, G., Schroder, M., & Woodgate, R. A. (1998). Gradual warming of the Weddell Sea Deep and Bottom Water, Filchner-Ronne Ice Shelf Program, Report No. 12. Bremerhaven, Germany: Alfred-Wegener-Institut, 24-34.

Fofonoff, P., & Millard, R. C. Jr. (1983). Algorithms for computation of fundamental properties of seawater, Unesco Tech. Pap. in Mar. Sci., 44, 53 pp.

Gille, S. (2002). Warming of the Southern Ocean since the 1950s. *Science*, *295*(5558). 1275–1277. https://doi.org/10.1126/science.1065863

Gille, S. (2008). Decadal-scale temperature trends in the Southern Hemisphere ocean. *Journal of Climate*, *21*, 4749–4765.

Gordon, A. L. (1975). An Antarctic oceanographic section along 170°E. *Deep Sea Research*, *22*, 357–377.

Hayakawa, H., Shibuya, K., Aoyama, Y., Nogi, Y., & Doi, K. (2012). Ocean bottom pressure variability in the Antarctic divergence zone off Lutzow-Holm Bay, East Antarctica. *Deep-Sea Research Part I*, *60*, 22–31.

Heywood, K. J., Sparrow, M. D., Brown, J., & Dickson, R. R. (1999). Frontal structure and Antarctic Bottom Water flow through the Princess Elizabeth trough, Antarctica. *Deep-Sea Research Part I*, *46*, 1181–1200.

Hirano, D., Kitade, Y., Ohshima, K. I., & Fukamachi, Y. (2015). The role of turbulent mixing in the modified shelf water overflows that produce cape Darnley Bottom Water. *Journal of Geophysical Research: Oceans*, *120*, 910–922. https://doi.org/10.1002/2014JC010059

Jacobs, S. S., & Georgi, D. T. (1977). Observations on the Southwest Indian/Antarctic Ocean. In M. Angel (Ed.), *A Voyage of Discovery*, edited by, (pp. 43–84). New York: Pergamon.

Jacobs, S. S., & Giulivi, C. F. (2010). Large multidecadal salinity trends near the Pacific-Antarctic continental margin. *Journal of Climate*, *23*, 4508–4524. https://doi.org/10.1175/2010JCLI3284.1

Johnson, G. C., Purkey, S. G., & Bullister, J. L. (2008). Warming and freshening in the abyssal southeastern Indian Ocean. *Journal of Climate*, *21*, 5353–5365.

Jullion, L., Garabato Naveira, A. C., Meredith, M. P., Holland, P. A., Courtois, P., & King, B. A. (2013). Decadal freshening of the Antarctic bottom water exported from the Weddell Sea. *Journal of Climate*, *26*, 8111–8125.

Jullion, L., Jones, S. C., Garabato Naveira, A. C., & Meredith, M. P. (2010). Wind-controlled export of Antarctic bottom water from the Weddell Sea. *Geophysical Research Letters*, *37*, L09609. https://doi.org/10.1029/2010GL042822

Kitade, Y., Shimada, K., Tamura, T., Williams, G. D., Aoki, S., Fukamachi, Y., et al. (2014). Antarctic Bottom Water production from the Vincennes Bay Polynya, East Antarctica. *Geophysical Research Letters*, *41*, 3528–3534. https://doi.org/10.1002/2014GL059971

Meijers, A. J. S., Klocker, A., Bindoff, N. L., Williams, G. D., & Marsland, S. (2010). The circulation and watermasses of the Antarctic shelf and continental slope between 30 and 80°E. *Deep Sea Research*, *2*(57), 723–737.

Menezes, V. V., Macdonald, A. M., & Schatzman, C. (2017). Accelerated freshening of Antarctic Bottom Water over the last decade in the Southern Indian Ocean. *Science Advances*, *3*, e1601426.

Meredith, M. P., Gordon, A. L., Naveira Garabato, A. C., Abrahamsen, E. P., Huber, B. A., Jullion, L., & Venables, H. J. (2011). Synchronous intensification and warming of Antarctic bottom water outflow from the Weddell Gyre. *Geophysical Research Letters*, *38*, L03603. https://doi.org/10.1029/2010GL046265

Meredith, M. P., Locarnini, R., Scoy, K. V., Watson, A., Heywood, K., & King, B. (2000). On the sources of Weddell Gyre Antarctic Bottom Water. *Journal of Geophysical Research*, *105*, 1093–1104.

Meredith, M. P., Naveira Garabato, A. C., Gordon, A. L., & Johnson, G. C. (2008). Evolution of the deep and bottom waters of the Scotica Sea, Southern Ocean, during 1995–2005. *Journal of Climate*, *21*, 3327–3343.

Nihashi, S., & Ohshima, K. I. (2015). Circumpolar mapping of Antarctic coastal polynyas and landfast sea ice: Relationship and variability. *Journal of Climate*, *28*, 3650–3670. https://doi.org/10.1175/JCLI-D-14-00369

Ohshima, K. I., Fukamachi, Y., Williams, G. D., Nihashi, S., Roquet, F., Kitade, Y., et al. (2013). Antarctic Bottom Water production by intense sea-ice formation in the cape Darnley Polynya. *Nature Geoscience*, *6*(3), 235–240. https://doi.org/10.1038/ngeo1738

Orsi, A. H., Johnson, G. C., & Bullister, J. L. (1999). Circulation, mixing, and production of Antarctic Bottom Water. *Progress in Oceanography*, *43*, 55–109.

Padman, L., Siegfried, M. R., & Fricker, H. A. (2018). Ocean tide influences on the Antarctic and Greenland ice sheets. *Reviews of Geophysics*, *56*, 142–184. https://doi.org/10.1002/2016RG000546

Purkey, S. G., & Johnson, G. C. (2010). Antarctic bottom water warming between the 1990s and the 2000s: Contributions to global heat and sea level rise budgets. *Journal of Climate*, *23*, 6336–6351.

Purkey, S. G., & Johnson, G. C. (2013). Antarctic bottom water warming and freshening: Contributions to sea level rise, ocean freshwater budgets, and global heat gain. *Journal of Climate*, *26*, 6015–6122.

Rintoul, S. R. (1998). On the origin and influence of Adélie land bottom water. In S. S. Jacobs, & R. Weiss (Eds.). *Ocean, Ice and Atmosphere: Interactions at Antarctic Continental Margin*, *Antarc. Res. Ser* (Vol. 75, pp. 151–171). Washington, D.C: AGU.

Rintoul, S. R. (2007). Rapid freshening of Antarctic Bottom Water formed in the Indian and Pacific Oceans. *Geophysical Research Letters*, *34*, L06606. https://doi.org/10.1029/2006GL028550l

Rye, C. D., Naveira Garabato, A. C., Holland, P. R., Meredith, M. P., Nurser, A. J., George, J., et al. (2014). Rapid sea-level rise along the Antarctic margins in response to increased glacial discharge. *Nature Geoscience*, *7*, 732–735.

Schmidko, S., Heywood, K. J., Thompson, A. F., & Aoki, S. (2014). Multi-decadal warming of Antarctic waters. *Science*, *346*(6214), 1227–1231. https://doi.org/10.1126/science.1256117

Schröder, M., & Fahrbach, E. (1999). On the structure and the transport of the eastern Weddell Gyre. *Deep-Sea Research Part II*, *46*, 501–527.

Tamura, T., Ohshima, K. I., Fraser, A. D., & Williams, G. D. (2016). Sea ice production variability in. *Antarctic coastal polynyas*, *121*, 2967–2979.

Thurnherr, A. M., Visbeck, M., Firing, E., King, B., Hummon, J., Krahman, G., & Huber, B. (2010). A manual for acquiring lowered Doppler current profiler data, IOCCP report no. 14, ICPO publication Series no. 134 Version 1, 21 pp.

Uchida, H., Katsumata, K., & Doi, T. (2015). WHP P14S, S04I Revisit in 2012 Data Book, 187pp, ISBN978–4–901833-21-9. https://doi.org/10.17596/0000030

van Wijk, E. M., & Rintoul, S. R. (2014). Freshening drives contraction of Antarctic bottom water in the Australian Antarctic Basin. *Geophysical Research Letters*, *41*, 1657–1664. https://doi.org/10.1002/2013GL058921

Vaughan, D. G., Comiso, J. C., Allison, I., Carrasco, J., Kaser, G., Kwok, R., et al. (2013). Observations: Cryosphere. In T. F. Stocker, D. Qin, G.-K. Plattner, M. Tignor, S. K. Allen, J. Boschung, A. Nauels, Y. Xia, V. Bex, & P. M. Midgley (Eds.), *Climate change 2013: The physical science basis. Contribution of working group I to the fifth assessment report of the Intergovernmental Panel on Climate Change* (Chap. 4, pp. 317–382). Cambridge, UK and New York, NY: Cambridge University Press.

Williams, G. D., Herraiz-Borreguero, L., Roquet, F., Tamura, T., Ohshima, K. I., Fukamachi, Y., et al. (2016). Suppression of Antarctic Bottom Water production by melting ice shelves in Prydz Bay, East Antarctica. *Nature Communications*, *7*(1), 1–9. https://doi.org/10.1038/ncomms12577